

Water trickling and roof falling of soft argillaceous roadways with its composite supporting and repairing technology

Wenyu Lv^{1, 2*}

¹School of Energy Engineering, Xi'an University of Science and Technology, Xi'an, 710054, China

²Technology Centre, Sichuan Coal Industry Group Co., Ltd., Chengdu, 610091, China

Received 6 October 2013, www.tsi.lv

Abstract

Using methods such as the transient electromagnetic method, rock mechanics testing, X-ray diffraction analysis, rock strength weakening experiment, borehole observation technology and grout mix design, etc. to study the mechanism of water trickling and roof falling of soft argillaceous roadways, via model analysis and numerical calculations, we reached many conclusions: Rock breakage is perpendicular to the axis of borehole; expansion of argillaceous swelling rock weakens the surrounding rock, the strength degradation of which occurs in 1h; performance of anchor agent also significantly decreased; uniaxial compressive strength, friction angle and cohesion of surrounding rock decreased by 40%, 16.5% and 11.1%, respectively; water trickling further exacerbated the risk of roof falling in the construction of roadway; according to calculation, the weak plane of the original 12 # I-beam became shear failure, and cannot meet the large initial deformation of roadways, floor heave is large with serious water logging. We presented the technology of "targeted drainage, deep-and-shallow hole grouting, advanced ductile, floor anchor rope, U29-shaped steel, and anchor net spray composite support". Site monitoring on 1# railway cross-cut of Bofang Coal Mine displayed that the maximum amount of deformation was less than 125mm, working resistance of anchor bolt and cable were 72-91kN and 123.3kN, respectively. Water trickling and roof falling were controlled; water logging of floor heave was improved obviously. Numerical simulations show that plastic zone is greatly reduced, and support effects were fairly good.

Keywords: soft and argillaceous, X-ray, water trickling and roof falling, composite support, numerical simulation

1 Introduction

For a long time, soft rock roadway support has been the difficulty of coal mine roadway support. China has made considerable progress in the research of soft rock control theory and basic theory of soft rock [1]. However, many research results have been concentrated on broken soft rock and high stress soft rock [2-4], while research of soft rock on argillaceous rock under water conditions has not been taken seriously and promoted high enough. Taken 1# railway crosscut of BoFang coal mine as engineering background, this paper studied the water trickling, roof falling, support and repair process of argillaceous roadways.

2 Engineering situations

2.1 GEOLOGICAL CONDITIONS

Buried depth of 1# railway crosscut is 39 m ~ 150 m and floor-elevation is +1401m, direction of drift driving is parallel with the shaft orientation, and its opening segment is located in the floor of 6-2 coal Seam. 1# railway crosscut passed through each coal seam and its surrounding rocks are mostly silty mudstone, argillaceous siltstone, siltstone and mudstone. The surrounding rocks have developed joints and fissures with strong water

conductivity. No significant water blocking layer overlying, roadway construction is largely affected by trickling water in the roof. Roadway layout near 1# railway crosscut is shown in Figure 1.

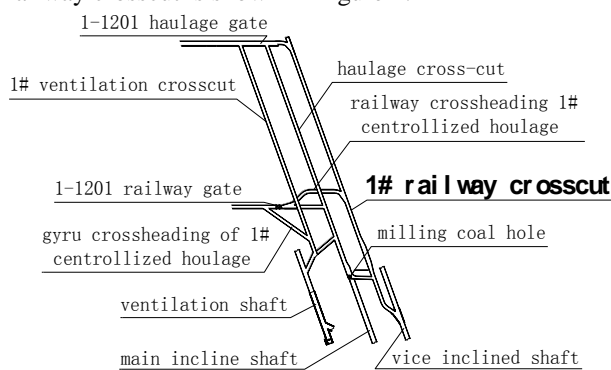


FIGURE 1 Roadway layout nearby 1# railway crosscut

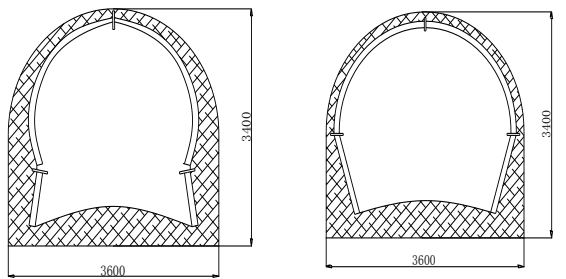
2.2 SUPPORTING SITUATION

1# railway crosscut is a roadway with the width 3.6m, height 3.4m, straight wall semi-circular cross-section. Support pattern is 12 # I-beam for mining (shield distance 800mm) + double-network + jet C20 concrete, railway steel (shield distance 800mm) + double-network+ jet C20 concrete. Deformation and damage of 1# railway crosscut is serious in original support. In the 43 days from January

* Corresponding author e-mail: lvwenyu2816@126.com

20, 2014 to March 4, the largest two sides move quantity of the middle yard segment (70 m~ 110 m from the opening) reached 1800 mm and the kick drum was serious; the largest convergence between roof and floor in this segment reached 1600 mm. Roadway's sides swelling out and roof subsidence were also serious, concrete in vault and shoulders cracked, and connections of steel support broke. Most of the bolt trays were very loose and the anchorage performance of anchor agent significantly reduced [5].

After the destruction of the top support connection, support was like "人" shape under pressure from the two sides. The connections of straight leg segments broke when the pressure from one side was greater. The insertion length of the leg reached 800 mm when pressure from roof was greater. Sketch of deformation and failure in 1# railway crosscut is shown in Figure 2.



a) leg of support broken b) leg of support move inward
 FIGURE 2 The sketch map of the deformation and failure

2.3 GENERAL SITUATION OF WATER TRICKLING, ROOF FALLING AND GEOPHYSICAL EXPLORATION

Roof collapse happened when 1# railway crosscut dug 124 meters in. The caving length was 7.8 meters, the largest caving height was 5.6 meters, and the caving position was 12.3 meters away from the driving face. While water trickling was serious before and rear the caving zone, but there was not a lot of water during excavation [6, 7]. This shows that serious water trickling was mainly due to the fractures generated when digging roadway, and these fractures were connected to the water bodies.

Considering that drilling method will produce a great impact on roadway excavation, after the roof falling, the geophysical prospecting has been done in the working face of 1# railway cross-cut with an YCS160 intrinsically safe transient electromagnetic instrument (TEM). There are 39 dates from 1 (working face) × 13 (view angle) × 3(direction) and the three directions were bottom, top and along driving direction, detection was along rock and floor direction and probing direction was 45° upward the level of the roof. Its apparent resistivity contour lines pseudosection (achievement) was shown in Figure 3.

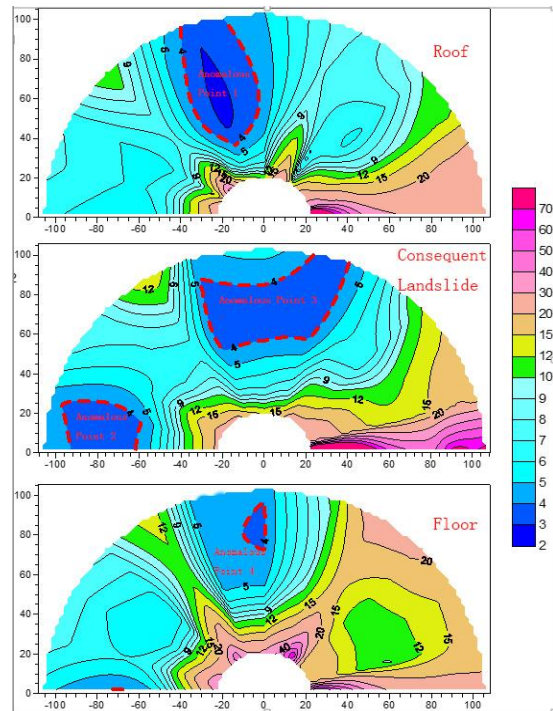


FIGURE 3 Apparent resistivity contour lines pseudosection (achievement) map of 1# railway cross-cut

In this figure, the values in the contours represent the conductive strength of underground rock. The higher the value is, the weaker the conductivity is. The smaller the value is, and the stronger the conductivity is. Detection conclusions are as follows based on the detection results: Roof direction detection results, abnormal point 1: abscissa -35 ~ -5m, ordinate 35 ~ 95m. Detection results along driving direction, abnormal point 2: abscissa 90 ~ -60m, ordinate 3 ~ 25m; abnormal point 3: abscissa -30 ~ 40m, ordinate 50 ~ 95m. Bottom direction detection results, abnormal point 4: abscissa -10 ~ 5m, ordinate 70 ~ 90m. Apparent resistivity is relatively low and water-abundance is better. We hypothesized that the water is from the water bearing structure, and also may be caused by water in the drilling process. Apparent resistivity is relatively high in other detection zone. In order to provide reliable data for repair scheme, surrounding rock components analysis and borehole observation also have been done in the following.

3 Surrounding rock components analysis

3.1 X-RAY DIFFRACTION EXPERIMENT

The mineral composition of soft rock is the key factor that determines its mechanical properties, according to the engineering characteristics of large water and roof fall project in 1# railway crosscut. Mechanical test and X-ray detection on representative rock samples in roof falling zone have been done. X-ray diffraction instrument was D/Max-3B. A diffraction pattern is shown in Figure 4, the main components are indicated and concrete components are given in Table 1.

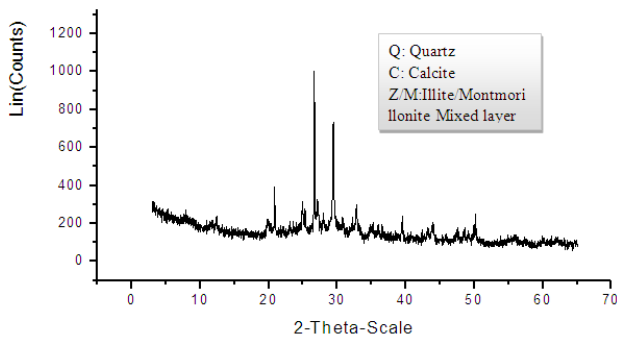


FIGURE 4 X-ray diffraction pattern

TABLE 1 experimental results of X ray diffraction

Sample No.	1#	2#	3#	4#	5#
Main Components	I/S, Q, C	I/S, Q, K, S	Q, K, D, S	I/S, Q, D, K	Q, S, K

Table: I/S: illite/montmorillonite mixed layer; Q: quartz; C: calcite; K: kaolinite; S: siderite; D: dolomite

3.2 SURROUNDING ROCK COMPONENTS ANALYSIS

The main components of the surrounding rock are: illite/montmorillonite mixed layer, quartz, calcite, kaolinite, siderite and dolomite [8], among which the kaolinite and illite belong to clay shale swelling rock, volume of this two kinds of rocks increase smaller when influenced by water, water can only weaken the connection force between particles. And montmorillonite expands when there is water, its volume change greatly resulting in the weakening of roadway surrounding rock.

1# railway crosscut is layout in the aquifer, joint and fracture of its surrounding rocks developed and water conductivity of the rock is also very good. Deformation characteristics are sensitive to moisture content [9]. The water content of this natural rock is 16.82% and saturated moisture content of this kind of rock is only 17.03%, though moisture content increased only 0.21% from natural state to saturation state, the uniaxial compressive strength decreased 40 percent, friction angle decreased 16.5%, and cohesion decreased 11.1%, as shown in Figure 5.

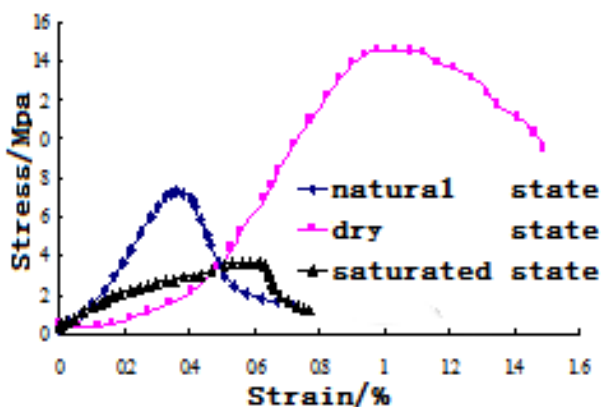


FIGURE 5 The effect of weakly cemented soft rock stress-strain curve

3.3 WEAKEN DEGREE OF MUDSTONE STRENGTH IN WATER

Take mudstone and argillaceous siltstone samples without flooding from the roadway to do the strength test in soaking in water.

In order to study the degree and speed of the impact of water on the mudstone rocks, the time interval is 60min and the results is shown in Figure 6.

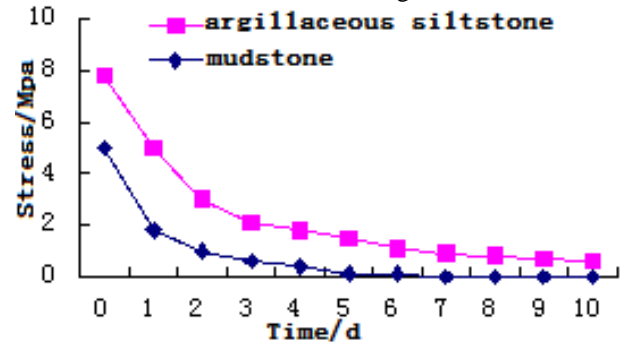


FIGURE 6 Attenuation curve of rock immersion strength

As seen from the figure, strength of the mudstones soaked in water decreases rapidly, and the water can decay the mudstones within a few hours. Strength degradation occurs mainly within the first 1h, less strength degradation occurs in 1-4h and strength will remain at 0.4MPa after 6 ~ 7h. At the same time, minerals that has cementation functionary in original rock will drain with the leaking water, and the anchorage performance of anchor agent significantly reduced.

4 1# railway crosscut surrounding rock structure detection

In order to detect the lithology, thickness, faults, fractures and other geological structure and their changes in roadway fracture development ring, the structure of 1# railway crosscut was probed with a YTJ20 rock drilling detector. The rock destruction within each borehole was shown in Figure 7 along the drilled axially from the inside out, in which drilling peep of 2# drilling was shown in Figure 8.

1) 1# railway crosscut is located in the stress concentration area which is in the transition section of topsoil to bedrock. By the drilling peep we can know the surrounding rocks are mostly silty mudstone, argillaceous siltstone, siltstone and mudstone. The surrounding rock has developed joints and fissures, and the structure is also very bad and rock cleats are disordered. Small structures were found during roadway excavation, no significant water blocking layer overlying, water trickling further exacerbated the danger of roof cave.

2) Through comprehensive analysis of the situation of each borehole peep, we discovered that within the range of 1.2 ~ 1.5m depth surrounding rock was severely broken. This range can be considered as broken loose body with lower bearing strength.

3) By monitoring the greatest damage depth from drilling peep, we know that damage within 3.65m was more serious; and with the increase of the drilling depth, rock destruction is easing. Therefore, it can be considered that the failure depth of roadway surrounding rock is 3.6m.

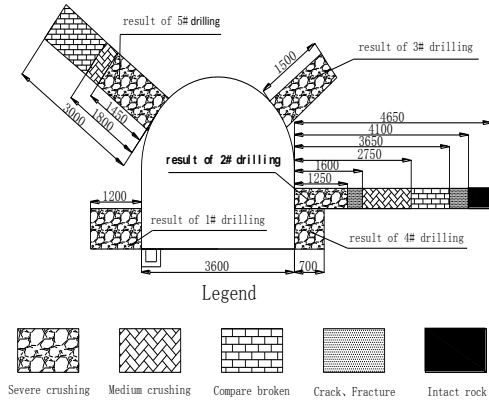


FIGURE 7 Distribution map of broken rock zone

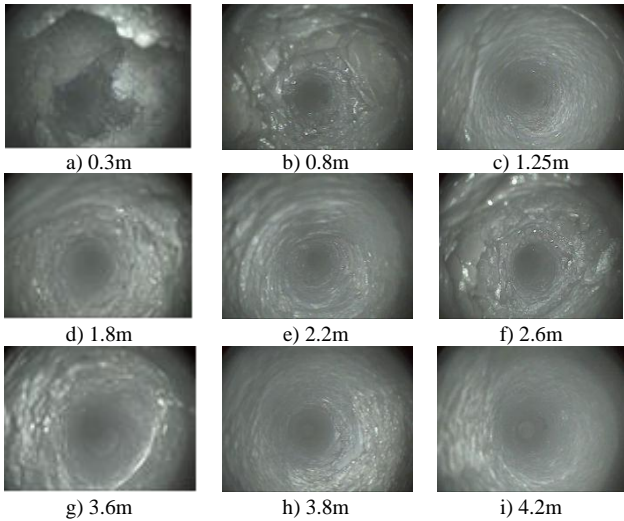


FIGURE 8 Picture of borehole peep

4) Through detection, we know that fracture is mainly caused by roadway excavation and lack of supporting strength. Most of the fractures are perpendicular to the borehole axis direction. The original support cannot guarantee the stability of surrounding rock, so the original support is failure.

5 1# railway crosscut repair scheme

5.1 SUPPORT PARAMETERS BASED ON MATHEMATICAL MODEL

5.1.1 Failure depth of the two walls and roof

By natural equilibrium arch theory, failure depth of the two walls was calculated by Equation (1):

$$C = \left(\frac{K_{cx} \gamma H B}{10^4 f_y} - 1 \right) h \tan \frac{90^\circ - \varphi}{2}, \tag{1}$$

where

K_{cx} – the surrounding rock extrusion stress concentration coefficient, determined by the cross-section shape and aspect ratio of roadway;

γ – the average gravity density from the roadway to the surface, kN/m^3 ;

H – depth from the roadway to the surface, (m);

B – dimensionless parameter represents the influence degree of mining;

f_y – coefficient of rock hardness, (m);

φ – internal friction angle of surrounding rock, ($^\circ$).

According to the relevant data of BoFang coal mine, the roadway side failure depth $C=0.56\text{m}$. The damage depth of roof strata b can be calculated according to Equation (2):

$$b = \frac{(a + C) \cos \alpha}{k_y f_n}, \tag{2}$$

where

a – half width of roadway, (m);

α – coal seam dip angle;

k_y – stability coefficient of the to be anchored rock;

f_n – coefficient of hardness of the anchored rock;

According to the relevant data of BoFang coal mine, failure depth $b=0.92\text{m}$.

5.1.2 Roof pressure

The calculation formula for the roof pressure according to the normal of rock beddings is:

$$Q_H = 2\gamma_n a b B = 83.13 \text{ kN/m}. \tag{3}$$

Roadway width is 3.6 m, and then the pressure of bracket is:

$$P = 2a Q_H = 299.25 \text{ kN}. \tag{4}$$

5.1.3 Carrying capacity

Calculation of bearing capacity of rail steel support and 12# I-steel support in 1# railway crosscut:

$$P_{18} = \sum_{i=1}^n Q_i L_i = Q_a \times \frac{\theta_2}{180} \times 3.14 + 2 \times Q_b L_b = 111.8 \text{ kN}. \tag{5}$$

$$P_{12} = \sum_{i=1}^n Q_i L_i = Q_a \times \frac{\theta_2}{180} \times 3.14 + 2 \times Q_b L_b = 223.02 \text{ kN}. \tag{6}$$

Calculation of bearing capacity of U29 type steel bracket under the same conditions:

$$P = \sum_{i=1}^n Q_i L_i = Q_a r \times \frac{180}{180} \times \pi + 2 \times Q_b t = 406.89 \text{ kN}. \tag{7}$$

The results show that, the original 12# I-steel support and 18 kg/m rail steel support are all rigid metal support, the bearing capacity is lower than the required load and cannot adapt to the muddy roadway initial large

deformation, support welds are weak and prone to shear failure. U29-type steel support is easy to connect, more flexible and easy in fabrication, the load-carrying capacity is 1.82 times of 12# I-steel and 3.64 times of 18 kg/m rail steel support and this can achieve the required load.

5.1.4 Repair scheme

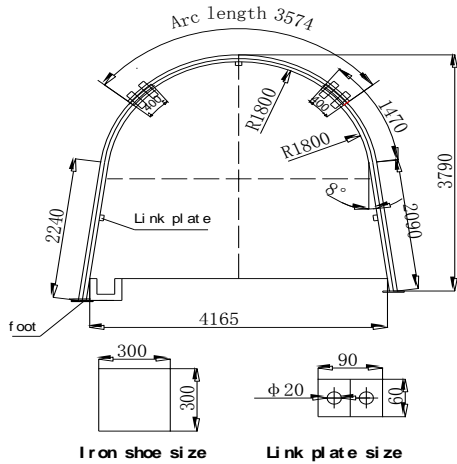


FIGURE 9 Design drawing of U-steel support

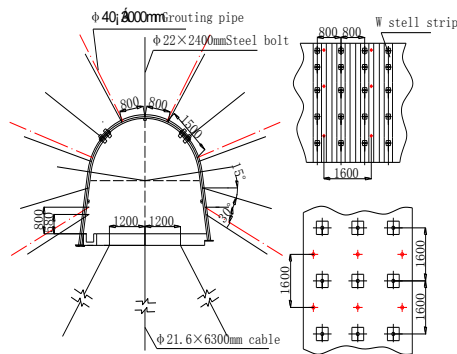


FIGURE 10 Orthographic views of combined support

TABLE 2 Tables of support parameters

Name	Parameters	
Bolt	Specifications	bolt specifications sinistral thread steel bolt with no longitudinal reinforcement Φ22×2400mm
	Length	1500mm
	Resin cartridge	K2335 one roll, Z2350 one roll
	Row & Line Space Number	800mm×800mm 11
Cable	Specifications of trays	200mm×200mm×10mm
	Cable specification	Φ21.6×6300mm
	Row & Line Space Number	1200mm×1600mm 3
Grouting Pipe	Specifications of trays	300mm×300mm×15mm
	Parameters	Φ40×3000mm, 1500×1600mm
Steel Strip	Model	W-type steel band (BHW-280-3.00)
Mesh Reinforcement	Material	Φ6steel, 1000mm×1500mm, mesh Size100mm×50mm

Through analysing the failure mechanism of 1# railway crosscut, we know that in the original support rock is broken, water trickling is serious with roof falling, roadway deforms severely and carrying capacity is low. The floor heave and waterlogging are serious, which is the sally port of the railway deformation. The two sides first broke under the stress caused by rock expansion, as the destruction continues the roof would also damage and finally the whole roadway broke. So we presented the technology of “targeted drainage, deep-shallow hole grouting, advanced conduit grouting, floor cable, U29-shaped steel anchor and net spray composite support” [10-13]. Cross-section design and orthographic views are shown in Figures 9 and 10, and bolt net support parameters is shown in Table 2.

5.2 GROUTING PARAMETERS

5.2.1 Slurry ratio parameter determines

In order to determine the ratio of grouting material, 425 # ordinary portland cement and 40 degrees Baume water glass (Formula Na₂O_nSiO₂) were used in laboratory experiment. The model is 7.07 × 7.07 × 7.07 cm cubes and stripping time is about 24 hours. After numbering the test blocks, these blocks would be maintained at constant temperature and humidity (about 20 Celsius), strength test was done on test blocks with a servo universal tester according to different age groups. The results are shown in Table 3.

TABLE 3 Grout setting time and intensity in different proportions

Groups	W:C	S:C	Setting time (min)	Strength (MPa)		
				The seventh day	The fourteenth day	
I	1:1	1:0.06	216	3.9	7.5	
	0.9:1		191	4.3	10.4	
	0.8:1		179	6.1	12.7	
	0.7:1		156	8.2	16.1	
	1:1		293	3.8	8.6	
II	0.9:1	1:0.05	245	4.1	10.7	
	0.8:1		229	6.3	14.3	
	0.7:1		210	8.3	16.7	
	1.0:1		327	5.1	9.6	
III	0.9:1	1:0.04	289	6.1	11.9	
	0.8:1		261	8.1	17.7	
	0.7:1		245	9.6	20.9	
IV	1.0:1	1:0.03	378	4.3	8.8	
	0.9:1		337	5.2	11.2	
	0.8:1		325	7.9	17.1	
			0.7:1	301	9.1	18.4

When cement and sodium silicate ratio S:C is 0.04:1 and water cement ratio is 0.7:1, the strength of test blocks is high. Considering strength, gel time, slurry pump and other factors, cement and sodium silicate is identified as S: C 0.04:1, water cement ratio (0.7~1).

5.2.2 Depth and row & line space of grouting hole

Empirical equation of rock fracture degree:

$$r_y = (0.78 + 2.13\gamma H / R_c) a, \tag{8}$$

where:

- γ – rock density;
- H – buried depth of roadway;
- R_c – strength of rock mass;
- a – roadway radius.

Cement grout can be only injected in the rock crack, which is more than 0.2 mm in width. Through calculation, the fissure development range of 1# railway crosscut is 3.7 m, the depth of grouting hole should be not less than 1.5~2.0m considering the permeability of rock. In addition, considering the permeability region of grout determining the depth of grouting hole 3500 mm

For the convenience of construction, grouting hole spacing is often designed the integer times to bolt spacing or metal support spacing. And penetrating distance of two grouting holes should have some overlap.

Grout diffusion distance is 0.5~3.0 m in field test of grouting, the design of grouting hole spacing and single hole diffusion distance roughly the same, and here is 1.5 m.

5.2.3 Determining the grouting pressure

A large number of experiments show that grouting pressure is generally less than 2 Mpa if grouting hole depth is limited and rock fissures are developed. To prevent rock splitting damage caused by grouting, grouting pressure cannot exceed 1/10 of rock's compressive strength in soft rock. Comprehensive consideration suggests that the grouting pressure was 3 MPa.

5.2.4 Targeted drainage and deep-shallow hole grouting

Targeted drainage: grouting before drainage to close the cracks, and after to cement fractured rock timely, crowd out the remaining water, fill the fractures caused by rock dehydration, reduce the attenuation of rock strength after water, improve the cohesion, angle of internal friction and tensile strength of rock, and finally improve the overall performance of rock compressive to maintenance the stability of roadway.

Shallow hole grouting: low-pressure grouting was used in shallow hole in order to consolidate the large fissures in shallow first and form a grout layer in the rock surface [14].

Deep grouting: deep hole grouting was conducted after forming a grout layer in shallow, this will enhance the bearing capacity of the roadway in a large range.

5.3 THE SUPPORTING EFFECT MONITORING

After the application of the control technology in BoFang coal mine, observation of roadway surface displacement and stress testing of anchor and cable were done. The results were shown in Figures 11 and 12.

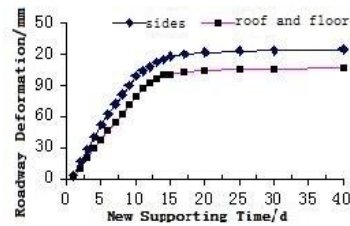


FIGURE 11 Surface displacement of roadways

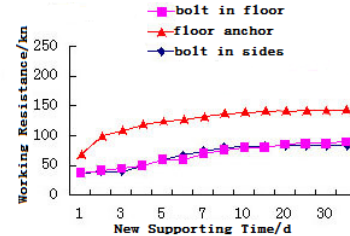


FIGURE 12 Resistance detection of bolt and anchor cable

1) Surface displacement of roadway [15, 16]. The maximum deformation of roadway sides was 124mm after the adoption of new supporting technologies and the maximum deformation of the roof and floor was 102mm; roadway deformation rate is relatively large in the former 12 days of support, the deformation rate of roadway was significantly lower 12 days later, and 15 days later the roadway was basically stable. 40 days after the introduction of new support technology, the surrounding rock has been stabilized.

2) Working resistance of cable and bolt. Initial support resistances of bolts and cables were about 36kN and 71kN respectively. The bolt support resistance grew significantly in the previous five days, and cable resistance had more growth in the previous 10 days. Surrounding rock was stable in 30 days, and support resistances of bolts and cables are 72-91 kN and 123.3 kN respectively. Floor support was strengthened, the two sides and roof deformation was prevented and the water condition has remarkable improved.

6 Numerical calculations based on FLAC3D model

The deepest point of 1# railway crosscut is 150m. Due to the complex geological conditions incurred by faults and complicate mechanical calculation of the stability of the surrounding rock [17], it is unable to carry on accurate analysis of the stability. This section mainly uses FLAC3D model to establish the expanding brush repair model (U-shape steel+ top slope bolt+ floor cable+ grouting model) [18, 19] to simulate plastic zone distribution of roadway surrounding rock in order to test the support effect. The result is shown in Figure 13.

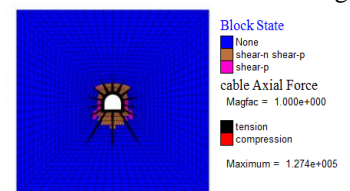


FIGURE 13 Plastic zone distribution of roadway

By calculating we concluded that the boundary of the upper part of the plastic zone is 1.37 m from the roof, the boundary of the lower part is 2.69m from the floor, boundary of the left part is 1.35m from the left side and boundary of the right part is 1.30m from the right part. The width of plastic zone of the two sides is shorter, and the scope of plastic zone is greatly reduced after the use of bolts and cables. Force of bolts and cables is relatively reasonable after using the repair program, in which the largest axial force of bottom cable is 127.4 kN. And the tails of anchoring segment are in the outside of the plastic zone of surrounding rock.

7 Conclusions

1) The surrounding rock of 1# railway crosscut contains mainly illite, montmorillonite and kaolinite, so the rock is easy to soften, fragmentation, collapse and swelling in water, resulting in the weakening of rock structure.

References

- [1] He Man-chao, Jing Hai-he, Sun Xiao-ming 2000 Research Progress of Soft Rock Engineering Geomechanics in China Coal Mine *Journal of engineering geology* **1** 46-62 (In Chinese)
- [2] Kang Hong-pu, Wang Jin-hua, Lin Jian 2007 High pretensioned stress and intensive bolting system and its Application in deep roadways *Journal of China Coal Society* **12** 1233-8 (In Chinese)
- [3] Sun Jun 1998 Research of rock mechanics on the joint of the century *Proceedings of the 5th Science conference of Chinese society for rock mechanics and engineering Chinese Science and Technology Press: Beijing* (In Chinese)
- [4] He Man-chao 1993 Survey of soft rock tunnel engineering Xuzhou: China university of Mining and technology press (In Chinese)
- [5] Zeng You-fu, Wu Yong-ping, Lai Xing-ping 2009 Analysis of roof caving instability mechanism of large-section roadway under complex conditions *Journal of Mining & Safety Engineering* **26**(4) 423-7 (In Chinese)
- [6] Xu Xing-liang, Zhang Nong 2007 Study of control process deformation behavior and of soft rock drift under rich water condition *Journal of China University of Mining & Technology* **36**(3) 298-302 (In Chinese)
- [7] Gou Pan-feng, Chen Qi-yong, Zhang Sheng 2004 Influence analysis of the anchor-hold of the resin bolt by the draining water in the drill hole *Journal of China Coal Society* **29**(6) 680-3 (In Chinese)
- [8] Liu Chang-wu, Lu Shi-liang 2001 Research on mechanism of mudstone degradation and softening in water *Rock and Soil Mechanics* **21**(1) 28-31 (In Chinese)
- [9] Gamboa E, Atrens A 2003 Environmental influence on the stress corrosion cracking of rock bolts *Engineering Failure Analysis* **10**(5) 521-58
- [10] Williams J H, Johnson C D 2004 A coustic and optical borehole-wall imaging for fractured-rock aquifer studies *Journal of Applied Geophysics* **55**(1) 151-9
- [11] Jiang Yao-dong, Zhao Yi-xin, Liu Wen-gang 2004 Research on floor heave of roadway in deep mining *Chinese Journal of Rock Mechanics and Engineering* **23**(14) 2396-2401 (In Chinese)
- [12] Pan Yi-shan, Zhu Ping, Wang De-li 1988 The creep simulation test and numerical analysis on deep roadway floor heave and its Prevention *Journal of Heilongjiang Mining Institute* **8**(2) 1-7 (In Chinese)
- [13] Marti J, Cundall P A 1982 Mixed discretization procedure for accurate solution of plasticity problems *International Journal for Numerical Methods in Engineering* **6** 129-39
- [14] You Chun-an 2004 Mechanics analysis of anchorage segment of pressure-type cable *Chinese Journal of Geotechnical Engineering* **26**(6) 828-31 (In Chinese)
- [15] Yang Xi-an, Hung Hong-gei, Liu Bao-wei 2000 Study on the deformation and support of weak rock mass roadway in the Jinchuan nickel mine *Journal of Xiangtan Mine Institute* **15**(3) 12-7 (in Chinese)
- [16] Wang Lian-guo, Li Ming-yuan, Wang Xue-zhi 2006 Study on mechanisms and technology for bolting and grouting in special soft rock roadways under high stress *Chinese Journal of Rock Mechanics and Engineering* **25**(16) 2889-94 (in Chinese)
- [17] Kang Hong-pu, Lin Jian 2001 New development in geomechanics measurement and test technology of mine roadway surrounding rock *Coal Science and Technology* **29**(7) 27-30 (In Chinese)
- [18] Lv Jun, Hou Zhong-jie 2000 Factors that influence the behavior of ground pressure under shallow conditions *Ground Pressure and Strata Control* **2** 39-43 (In Chinese)
- [19] Li Shu-qing, Wang Wei-jun, Pan Chang-liang 2006 Numerical Analyses on Support Structure of Rock around Deep Roadway *Chinese Journal of Geotechnical Engineering* **28**(3) 377-81 (In Chinese)

Authors



Wenyu Lv, born in May, 1981, Xian City, Shanxi Province, China

Current position, grades: the Lecturer of School of Xi'an University of Science and Technology, China.

University studies: Ph.D. degree in Mining Engineering from China University of Mining & Technology Beijing in China.

Scientific interest: Computer application in coal mining, backfill mining technology.

Publications: More than 20 papers published in various journals.

Experience: teaching experience of 3 years; 3 scientific research projects.